

Mutations derepressing silent centromeric domains in fission yeast disrupt chromosome segregation

Robin C. Allshire,¹ Elaine R. Nimmo, Karl Ekwall, Jean-Paul Javerzat, and Gwen Cranston

MRC Human Genetics Unit, Western General Hospital, Edinburgh, EH4 2XU, Scotland, UK

The *ura4*⁺ gene displays phenotypes consistent with variegated expression when inserted at 11 sites throughout fission yeast centromere 1. An abrupt transition occurs between the zone of centromeric repression and two adjacent expressed sites. Mutations in six genes alleviate repression of the silent-mating type loci and of *ura4*⁺ expressed from a site adjacent to the silent locus, *mat3-M*. Defects at all six loci affect repression of the *ura4*⁺ gene adjacent to telomeres and at the three centromeric sites tested. The *clr4-S5* and *rik1-304* mutations cause the most dramatic derepression at two out of three sites within *cen1*. All six mutations had only slight or intermediate effects on a third site in the center of *cen1* or on telomeric repression. Strains with lesions at the *clr4*, *rik1*, and *swi6* loci have highly elevated rates of chromosome loss. We propose that the products of these genes are integral in the assembly of a heterochromatin-like structure, with distinct domains, enclosing the entire centromeric region that reduces or excludes access to transcription factors. The formation of this heterochromatic structure may be an absolute requirement for the formation of a fully functional centromere.

[Key Words: *S. pombe*; PEV; heterochromatin; telomere; mating type]

Received October 7, 1994; revised version accepted December 13, 1994.

The centromeres of the fission yeast *Schizosaccharomyces pombe* are complex structures composed of large repetitive arrays symmetrically arranged around a nonrepetitive central domain (Hahnenberger et al. 1991; Murakami et al. 1991; Takahashi et al. 1992; Steiner et al. 1993; *cen1* is shown in Fig. 1A, below). Long arrays of tandem satellite repeats are frequently associated with the centromeres of many eukaryotes (Miklos and Cotsell 1990; Rattner 1991; Tyler-Smith and Willard 1993). These centromeric satellites are packaged into a highly compacted structure known as constitutive heterochromatin, but it is not known if this contributes to centromere function. It is likely that mammalian satellite repeats contribute to kinetochore formation, but alone, they may not be sufficient to form a functional centromere (Earnshaw et al. 1989; Haaf et al. 1992; Larin et al. 1994).

Genes placed in the vicinity of centromeric heterochromatin in mouse cells can exhibit variable states of expression (Butner and Lo 1986). This phenomenon, termed position effect variegation (PEV), was first described in *Drosophila*, where it was found that genes placed adjacent to centromeric heterochromatin were unstably repressed (Eissenberg 1989; Henikoff 1990; Karpen 1994). In *Drosophila*, mouse, and human cells, some

studies indicate that heterochromatin is often associated with the nuclear periphery (Hochstrasser et al. 1986; Ferguson and Ward 1992; Vourc'h et al. 1993). It is possible that this and other associations serve to lock these regions of chromosomes in an inactive state (Karpen 1994).

In unicellular organisms, such as yeasts, there are chromosomal regions with features characteristic of heterochromatin. The silent mating-type loci *HML* and *HMR* in the budding yeast, *Saccharomyces cerevisiae*, are normally maintained in a repressed state (for review, see Laurenson and Rine 1992), and genes placed close to telomeres are reversibly repressed (Gottschling et al. 1990). Mutations in the *RAP1*, *RIF1*, *ABF1*, *SIR1-SIR4* genes (for review, see Laurenson and Rine 1992) and components of the ORC (origin recognition complex; Bell et al. 1993; Foss et al. 1993; Micklem et al. 1993) act to reduce or abolish repression at the silent mating-type loci. In addition, mutations affecting the conserved amino-terminal region of histone H4 (*HHF1* and *HHF2*) and mutations in components of amino-terminal protein acetyltransferase (*NAT1* and *ARD1*) also affect silencing at the *HM* loci (for review, see Laurenson and Rine 1992). A subset of these mutations also relieve transcriptional repression at telomeres, whereas deletion of the *RIF1* gene enhances this repression (Aparicio et al. 1991; Kyriou et al. 1993). The *RAP1* protein and perhaps telomeres aggregate at the nuclear periphery (Klein et al. 1992; Palladino et al. 1993). This localization of *RAP1p*

¹Corresponding author.

is dependent on the products of the *SIR3* and *SIR4* genes, suggesting that they are involved in tethering RAP1p and maybe telomeres to the nuclear envelope (Palladino et al. 1993). These factors are therefore implicated in the assembly of the silent mating-type loci and telomeres into related heterochromatin-like structures that have variable accessibility to transcription factors and other proteins (Gottschling 1992; Singh and Klar 1992).

In fission yeast, genes placed within any of the three centromeres are transcriptionally repressed and exhibit phenotypic variegation (Allshire et al. 1994). As in many organisms, recombination across fission yeast centromeres is also suppressed (Nakaseko et al. 1986) and they contain large domains packaged into unusual chromatin (Polizzi and Clarke 1991; Takahashi et al. 1992). Fission yeast centromeres and telomeres, except during mitosis, are associated with the nuclear periphery throughout the cell cycle (Funabiki et al. 1993). Therefore, the centromeric regions of *S. pombe* chromosomes share many characteristics in common with heterochromatin and, although not visible by conventional staining methods, can be considered as representing small domains of centromeric heterochromatin. Centromeres are not the only regions of fission yeast chromosomes that have properties akin to heterochromatin. Reversible repression is also known to occur adjacent to the silent mating-type loci (*mat2* and *mat3*; Thon et al. 1994) and telomeres (Nimmo et al. 1994). Repression of the silent mating-type loci is alleviated by mutations at the *clr1*⁺, *clr2*⁺, *clr3*⁺, *clr4*⁺, *rik1*⁺, or *swi6*⁺ loci (Egel et al. 1989; Thon and Klar 1992; Ekwall and Ruusala 1994; Lorentz et al. 1994; Thon et al. 1994).

The *swi6*⁺ gene is nonessential and encodes a protein with homology to proteins containing a chromodomain (Lorentz et al. 1994) including the *Drosophila* heterochromatin protein HP1 (Powers and Eissenberg 1993), *Polycomb* (Paro and Hogness 1991), murine m31 and m32, and human HSM (Singh et al. 1991) and HP1^{Hsα} (Saunders et al. 1993). Mutant forms of *Drosophila* HP1 act as suppressors of variegating genes, whereas overexpression results in enhanced repression (Eissenberg et al. 1992). Several chromodomain proteins have been found associated with centromeric heterochromatin (Powers and Eissenberg 1993; Saunders et al. 1993; Nicol and Jeppesen 1994; Wreggett et al. 1994). Similarly, *Polycomb* is required to maintain repression of homeotic genes during development (Paro 1993).

The studies of telomeric silencing in *S. cerevisiae* suggested that some or all of the products of the *clr1*⁺, *clr2*⁺, *clr3*⁺, *clr4*⁺, *rik1*⁺, and *swi6*⁺ genes might be involved in silencing not only at the *mat* loci, but also at telomeres and centromeres in *S. pombe*. Here, we first establish the limits of the silenced domain within *S. pombe cen1* and test the effect of mutations at these six loci on *ura4*⁺ expression at various locations: adjacent to *mat3-M*, integrated at three sites within *cen1*, or next to a telomere. Three of the mutations identify gene products crucial for the maintenance of centromeric gene repression and/or complete centromere function. We propose that the formation of a heterochromatin-like struc-

ture is important for centromere function in fission yeast and utilizes factors involved in silencing at other chromosomal locations.

Results

The assays

In the data presented below, repression of the *ura4*⁺ gene at various sites in the fission yeast genome (centromeric, telomeric, adjacent to *mat3*) is assayed in two ways. First, all strains contain a convenient control *ura4-DS/E* minigene allele residing at the *ura4* locus that produces a truncated, nonfunctional, mRNA easily distinguishable from full-length *ura4*⁺ mRNA by Northern analyses. After quantitation, the ratio of the full-length *ura4*⁺ mRNA to the truncated minigene control mRNA allows the level of expression/repression from each site to be assessed. In all cases, these strains are grown under nonselective conditions so the level of *ura4*⁺ expression seen in each strain reflects an average for the whole population. The second assay is presented in the form of serial dilution of cells from each strain plated on nonselective (N/S), selective (URA⁻), or counterselective (FOA) plates. In fission yeast it is not known how much *ura4*⁺ product is required to render a cell Ura⁺. In addition, it is not known how much *ura4*⁺ product can be tolerated in an FOA-resistant cell. Previously, we have shown that strains with the *ura4*⁺ gene inserted within *cen1*, *cen2*, or *cen3* and grown in N/S, FOA, or URA⁻ media have the same repressed level of *ura4*⁺ message (Allshire et al. 1994). Therefore, there must be a relatively low threshold of *ura4*⁺ gene expression below which a cell is FOA resistant and above which it is Ura⁺ and FOA sensitive. The plating assays appear more sensitive to small changes in the level of *ura4*⁺ expression around this threshold. Northern analyses cannot always detect these small differences in expression but permit a distinction between slight alleviation and more dramatic derepressed states. In addition, some strains with the *ura4*⁺ gene inserted at certain centromeric sites have, on average, a high level of *ura4*⁺ expression but can form FOA^r colonies at a relatively high frequency. Closer examination often reveals that the colonies formed are smaller than colonies formed by control strains. A plausible explanation is that the *ura4*⁺ gene in such strains is generally expressed under nonselective growth conditions but that the repressed state is selected upon plating on FOA. These strains can be thought of as bearing a repressible *ura4*⁺ gene. Similarly, other strains that have low levels of *ura4*⁺ mRNA under nonselective growth conditions but that can grow on URA⁻ plates can be thought of as bearing an expressible *ura4*⁺ gene. The range of repression/expression of *ura4*⁺ at different sites of insertion is variable, presumably reflecting differential access to transcription factors at these sites.

Variegated expression of ura4⁺ occurs at multiple sites within cen1

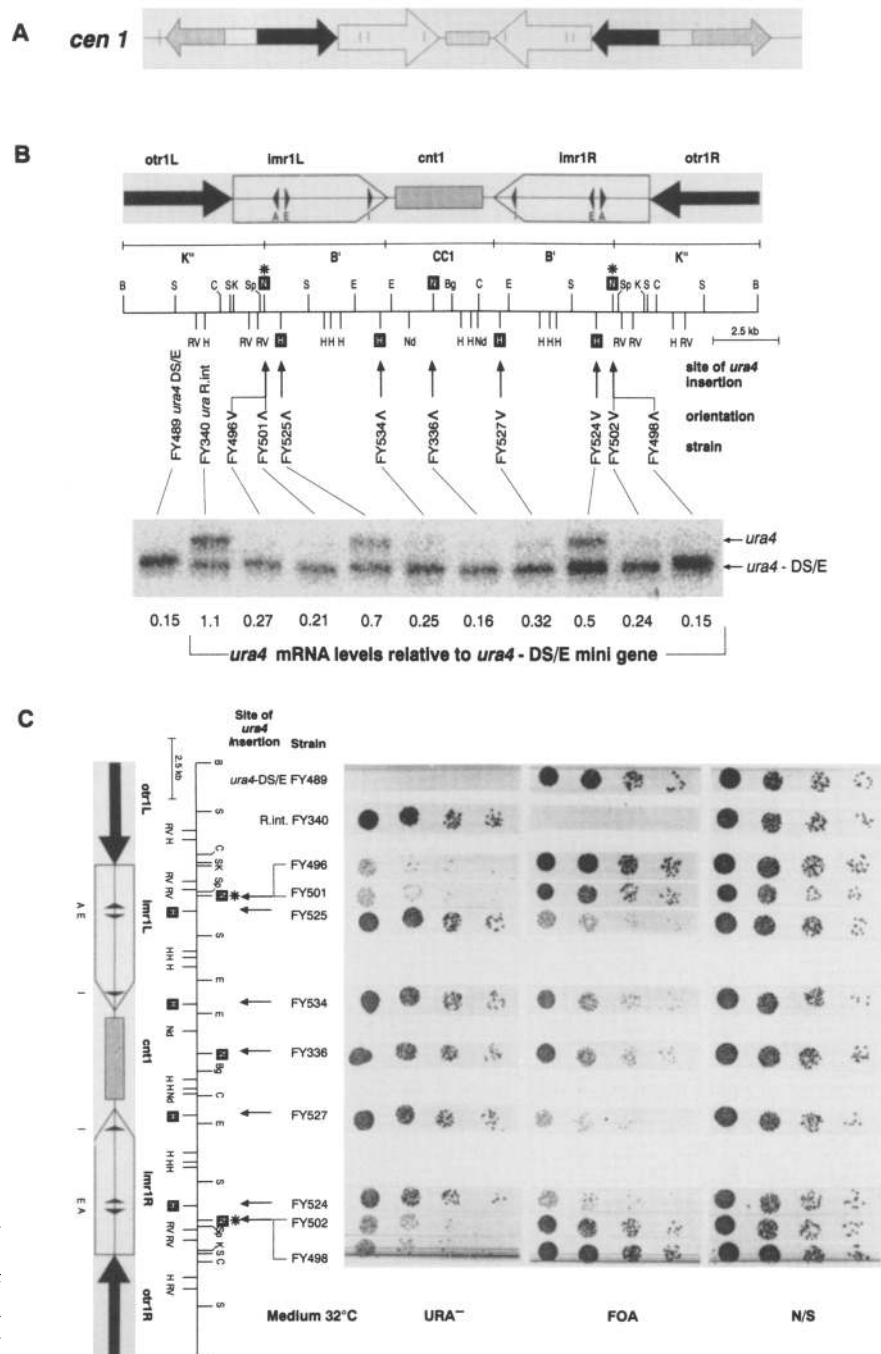
The *ura4*⁺ gene is variably repressed when placed at a

central location within fission yeast *cen1*, *cen2*, or *cen3* as judged by reduced levels of expression and heterogeneity in the ability to form colonies on selective (URA⁻) or counter selective (FOA) plates (Allshire et al. 1994). To establish the extent of the position-effected domain, further analyses have concentrated on the entire region of ~35 kb containing *cen1* (Fig. 1A).

The *ura4*⁺ gene was inserted at 13 sites within and immediately flanking the *cen1* region by transplacement with cloned fragments of *cen1* DNA disrupted by the *ura4*⁺ gene. Southern analyses indicated that in each case the structure of *cen1* was preserved, apart from the

desired *ura4*⁺ insertion event (data not shown). The *ura4*⁺ gene was first inserted at seven sites (shown in Fig. 1B,C) extending from the *NcoI* site on the left side of *imr1L* (B'), across *cnt1* (CC1) to the *NcoI* site at the right side of *imr1R*(B'). The *ura4*⁺ gene is shown inserted in both orientations at the left and right *imr1* *NcoI* sites. Only one orientation of the *ura4*⁺ gene is shown at the other insertion sites (Fig. 1B). Transcription of the *ura4*⁺ gene at each insertion site was examined by comparison with the *ura4-DS/E* minigene internal control (Allshire et al. 1994). Figure 1B shows a symmetrical profile with respect to *ura4*⁺ expression levels across *imr1L*, *cnt1*,

Figure 1. The insertion and state of repression of the *ura4*⁺ gene within the central region of *cen1*. (A) A schematic representation of *S. pombe* *cen1*. (B) Northern analyses of total RNA prepared from strains with the *ura4*⁺ insertion sites as shown grown in rich nonselective medium (YEA) at 32°C. The filter was hybridized with labeled *ura4-DS/E* probe washed and exposed to a PhosphorImaging screen. The resulting image is shown from which the relative level of *ura4*⁺ RNA produced from the intact gene vs. that from the *ura4-DS/E* minigene residing at the *ura4* locus was calculated (below tracks). The position of each *ura4*⁺ insertion relative to a restriction map and schematic diagram of the central region of *cen1* is shown. The nomenclature of various regions is as presented by Takahashi et al. (1992), and the K''/B'/CC1 nomenclature of Hahnenberger (1991) is also outlined. The vertical lines within the *imr1L* and *imr1R* regions show the position of tRNA genes. The symbols < and > indicate the direction of transcription of the inserted *ura4*⁺ gene at each site. The sites where the *ura4*⁺ gene was inserted in both orientations are marked (*). Restriction enzyme sites: (B) *Bam*HI; (Bg) *Bgl*II; (C) *Cl*aI; (E) *Eco*RI; (RV) *Eco*RV; (H) *Hind*III; (Hp) *Hpa*I; (K) *Kpn*I; (N) *Nco*I; (Nd) *Nde*I; (S) *Sph*I; (Sp) *Spe*I; (X) *Xho*I. (Not all sites for each enzyme are shown.) (C) Cultures of the same strains as shown in B above were grown to 0.5 × 10⁷ to 2.0 × 10⁷ cells/ml in N/S medium. Serial dilutions (1:5) of each culture were spotted onto URA⁻, FOA, and N/S plates and incubated at 32°C for 3–4 days. The highest density spots contained 4 × 10³ cells. Strains and location of the *ura4*⁺ gene within *cen1* are indicated with respect to the same schematic diagram as described in B.



and *imr1R*, reflecting the inverted arrangement of sequences in this region of the centromere. The *ura4⁺* gene is repressed at all sites but is apparently expressed well when placed between the tRNA^{ala} and tRNA^{glu} genes.

Growth of these strains at 32°C in the absence of uracil or presence of FOA is shown in Figure 1C. Again, there is a symmetrical relationship with respect to their ability to grow on URA⁻ and FOA plates. All strains grow equivalently on nonselective plates. Strains FY496, FY498, FY501, and FY502, with low levels of *ura4⁺* transcript under nonselective growth conditions, form more large colonies on FOA than on URA⁻ plates. However, strains such as FY524 and FY525, which show relatively high levels of *ura4⁺* transcription under nonselective conditions (0.5 and 0.7 in Fig. 1B), grow well on URA⁻ plates and poorly on FOA plates. In these strains the *ura4⁺* gene is inserted in the 350-bp region between two tRNA genes. It is known that this region of chromatin is DNase I hypersensitive (Takahashi et al. 1992); therefore, this site may also be more accessible to transcription factors. The fact that these strains can form small

colonies on FOA plates indicates that the *ura4⁺* gene at these sites is still repressible.

The *ura4⁺* gene was also inserted at four sites within *otr1* (*dg1/dh1* or *K'/L/K''*) and two sites just outside *cen1* (Fig. 2A). Insertion of *ura4⁺* into *otr1* was complicated by the fact that not only are there 2 copies of the repetitive elements comprising the *cen1 otr*, but *cen2* and *cen3* contain up to 4 and 13 copies of these repeats, respectively (Steiner et al. 1993). Consequently, insertion events at these sites within *cen1* were infrequent, and for this reason only left-side or right-side *otr1* insertion events were analyzed. Because of the symmetry of *cen1*, we assumed that the behavior at equivalent sites on each side would be identical. Only FY648 has the *ura4⁺* gene inserted on the right side, whereas all others are on the left as drawn. All insertion sites within *otr1* showed reduced *ura4⁺* mRNA levels (Fig. 2A). Even in strains FY939 and FY988, with insertion sites in the more distal region of *otr1*, expression of the inserted *ura4⁺* gene is still repressed and many colonies develop on FOA plates (Fig. 2B). However, just 0.9 and 1.2 kb outside *otr1*, at the *XhoI* (FY937) and *HpaI* (FY941) sites,

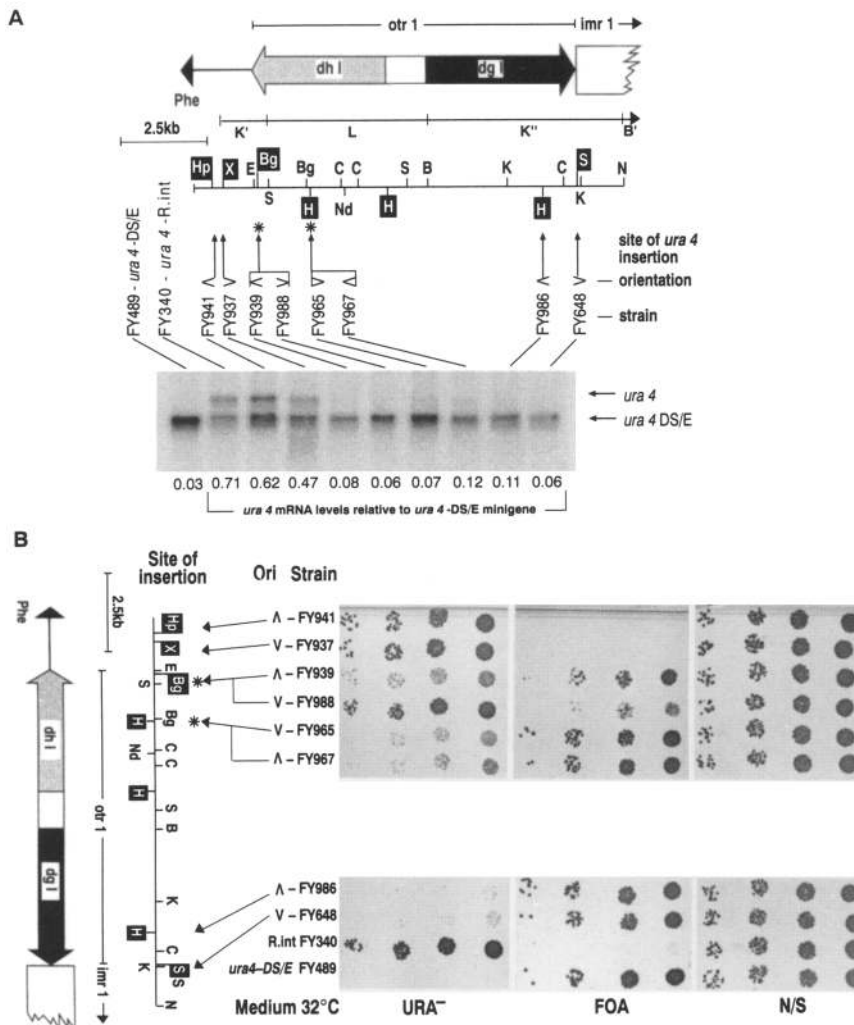


Figure 2. The insertion and state of repression of the *ura4⁺* gene within the outer regions of *cen1*. (A) Northern analyses of total RNA prepared from strains with *ura4⁺* insertion sites as shown grown in rich nonselective medium (YEA) at 32°C was performed as in Fig. 1B. The position of each *ura4⁺* insertion relative to a restriction map (enzyme abbreviations as in Fig. 1B, not all sites for each enzyme are shown) and schematic diagram of outer region of *cen1* is shown. The nomenclature of various regions is as presented by Takahashi et al. (1992), and the *K'/L/K''* nomenclature of Hahnenberger (1991) is also outlined. The position of Phe tRNA gene flanking *cen1* at left (Takahashi et al. 1992) is shown. The symbols < and > indicate the direction of transcription of the inserted *ura4⁺* gene at each site. The *ura4⁺* gene was inserted in both orientations at those sites marked (*). (B) Cultures of the same strains as shown in A above were grown to 0.5×10^7 to 2.0×10^7 cells/ml in N/S medium. Serial dilutions (1:5) of each culture were spotted onto URA⁻, FOA, and N/S plates and incubated at 32°C for 3–4 days. The highest density spots contained 4×10^3 cells. Strains and location of the *ura4⁺* gene within *cen1* are indicated with respect to the same schematic diagram as described in A.

the *ura4⁺* gene is expressed at relatively high levels (Fig. 2A) and colonies are rarely formed on FOA plates ($<1 \times 10^{-4}$; Fig. 2B).

These data suggest that there is a rapid change between the repressed region inside the distal *Bgl*III site in *otr1* to the expressing *Xho*I site 0.9 kb outside the centromeric domain. Repression of the *ura4⁺* gene outside the distal region of the large inverted repeat is minimal. Consistent with this abrupt transition in centromeric repression, plating experiments suggest that at the distal *Bgl*III insertion site the *ura4⁺* gene is more repressed when its promoter is adjacent to *otr1* (FY939) than when it is adjacent to the flanking outer sequences (FY988). Fewer and smaller FOA^r colonies result from the strain FY988 with the *ura4⁺* gene transcribed toward the centromere (Fig. 2B). No effect of gene orientation is seen at other sites where tested (cf. FY965 and FY967).

Mutations at six loci alleviate silencing of *ura4⁺* adjacent to *mat3* and telomeres

In *S. cerevisiae*, mutations in genes that suppress silencing at the silent mating-type loci also alleviate repres-

sion of telomere adjacent genes (Aparicio et al. 1991). Six previously isolated mutations, *clr1-5*, *clr2-E22*, *clr3-E36*, *clr4-S5*, *rik1-304*, or *swi6-115*, appear to alleviate repression of the *S. pombe* silent mating-type loci, *mat2-P* and *mat3-M* (Egel et al. 1989; Thon and Klar 1992; Ekwall and Ruusala 1994; Lorentz et al. 1994). When the *ura4⁺* gene is inserted adjacent to the *mat3-M* locus (*mat3-M::ura4⁺*) its expression is severely repressed, but this is alleviated by mutations at the *clr1*, *clr2*, *clr3*, *clr4*, *rik1*, and *swi6* loci (Ekwall and Ruusala 1994; Thon et al. 1994). Figure 3A demonstrates that the *mat3::ura4⁺* gene results in only a few small colonies on URA⁻ plates but many large colonies on FOA plates in a wild-type background. In contrast, the six mutant backgrounds reduce or lose this ability to grow in the presence of FOA and gain the ability to grow normally on URA⁻ plates. Control strains bearing the *ura4-DS/E* locus alone or in addition to a functional *ura4⁺* gene integrated at a random, nonrepressed site (Allshire et al. 1994) are included for comparison.

Transcription of the *mat3-M::ura4⁺* gene was compared with that from the *ura4-DS/E* minigene by Northern analyses (Fig. 3B). Very little *ura4⁺* transcript is de-

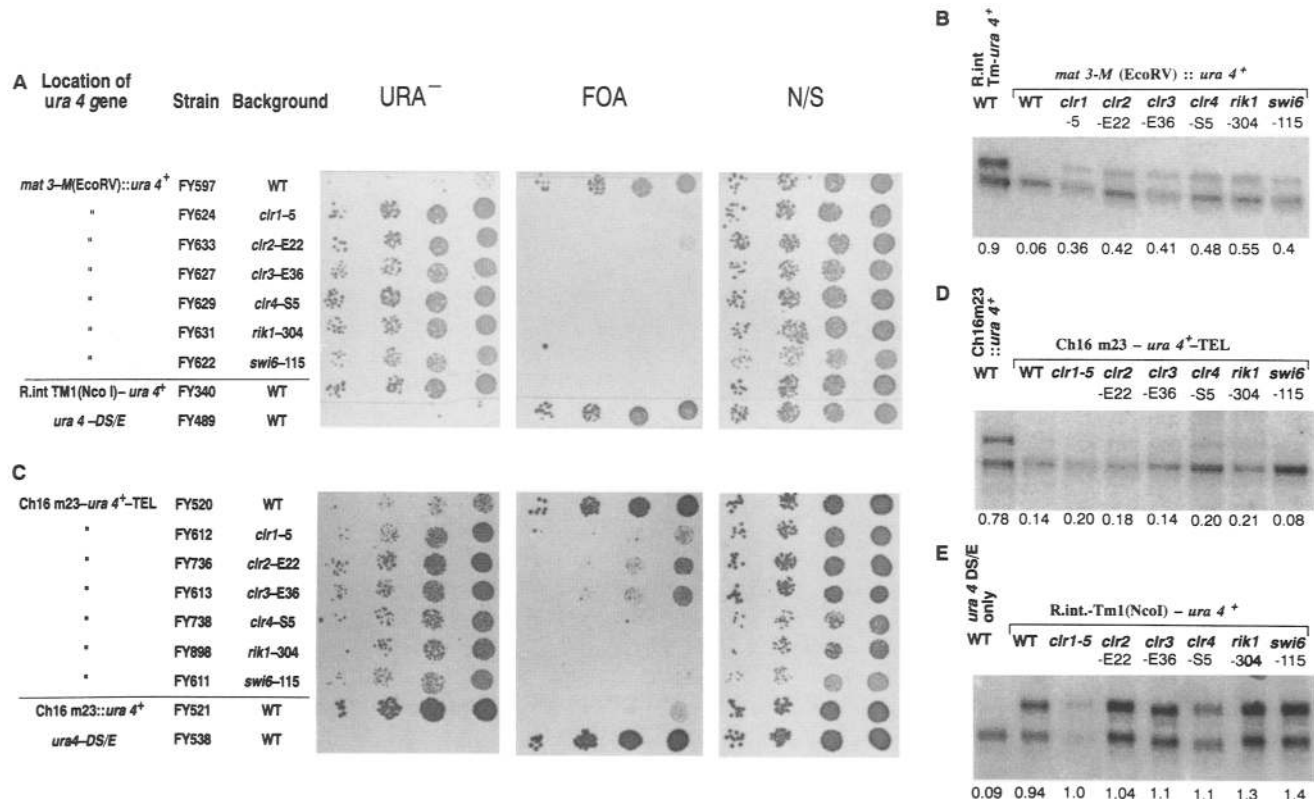


Figure 3. The effect of mutations at the *clr1*, *clr2*, *clr3*, *clr4*, *rik1*, and *swi6* loci on FOA resistance, uracil prototrophy, and expression of *ura4⁺* inserted next to *mat3-M* or adjacent to a telomere. Cultures with the *ura4⁺* gene borne next to *mat3-M* (A), a telomere (C) in wild-type and mutant backgrounds as shown, were grown to 0.5×10^7 to 2.0×10^7 cells/ml in N/S medium. Serial dilutions (1:5) of each culture were spotted onto URA⁻, FOA, and N/S plates and incubated at 32°C for 3–4 days. The highest density spots contained 4×10^3 cells. The same strains and one with the *ura4⁺* gene at an unknown random site in the genome (E) were grown in YEA-rich, nonselective medium at 32°C, total RNA was prepared and subjected to Northern analyses with labeled *ura4-DS/E* fragment as a probe (B,D,E). Quantitation of the resulting PhosphorImage is presented below.

tected in a wild-type background, but the presence of any of the six mutations increases the level of *ura4⁺* message to levels approximately half that of the minigene control. Thus, although these mutations suppress the ability of a *mat3::ura4⁺* strain to grow on FOA, they do not completely abolish all repression imposed on this *ura4⁺* gene. Complete deletion of the nonessential *swi6⁺* gene had identical effects as the *swi6-115* allele on expression from *mat3::ura4⁺* (data not shown).

The six mutations were also tested for their effect on telomere-mediated repression of *ura4⁺* using a strain with the gene adjacent to and transcribed toward a telomere constructed by telomere-associated chromosome breakage of a nonessential minichromosome Ch16 (Nimmo et al. 1994). Serial dilution assays and Northern blot analyses were performed (Fig. 3C,D). In the wild-type background, the telomere-adjacent *ura4⁺* gene (Ch16 m23-*ura4⁺*-TEL) is repressed, because this strain (FY520) displays reduced growth on URA⁻ plates, whereas many large colonies are visible on FOA plates. This situation is reversed by the presence of any of the six mutations, indicating that defects in any of these genes can alleviate the repressive effects imposed by the nearby telomere (Fig. 3C). However, the levels of *ura4⁺* transcript produced from the telomeric site indicate that these mutations have only slight effects on repression (Fig. 3D). Deletion of the entire *swi6⁺* gene had the same minimal effect on expression of this telomeric *ura4⁺* gene (data not shown). Therefore, none of the six mutations tested abolishes repression imposed by telomeres on the adjacent *ura4⁺* gene.

As a control, Northern analyses of a set of strains containing TM1-*ura4⁺* integrated at a random site (Allshire et al. 1994) in wild-type and mutant backgrounds is shown (Fig. 3E). The *ura4⁺* gene is expressed at normal levels, and none of the six mutations tested alters the expression of this *ura4⁺* gene.

The clr4 and rik1 mutations abolish ura4⁺ repression at certain sites within cen1.

Strains with mutations in any of the six genes were tested to see if they alter repression of *ura4⁺* genes inserted within fission yeast centromeres. Three sites of *ura4⁺* insertion within *cen1* (shown in Figs. 1 and 2) were analyzed: the central *NcoI* site within *cnt1/TM1* (FY336), the *NcoI* site at the right end of *imr1R* (FY498), and the *SphI* site in *otr1R* (FY648). Plating assays of strains bearing one of these insertion sites, the *clr1-5*, *clr2-E22*, *clr3-E36*, *clr4-S5*, *rik1-304*, *swi6-115*, or *swi6Δ::his1⁺* lesion, and the *ura4-DS/E* minigene control are shown in Figure 4. Wild-type controls and strains with a randomly integrated *ura4⁺* gene or no functional *ura4⁺* gene are included.

Most mutations alleviate *ura4⁺* repression regardless of the site of insertion in the centromere, as shown by the impaired ability of these *cen1 ura4⁺* insertion strains to form colonies on FOA plates. This suggests that the level of expression from *ura4⁺* genes inserted within the centromere, at any of the sites tested, may

increase when there is a defective *clr1*, *clr2*, *clr3*, *clr4*, *rik1*, or *swi6* gene. Mutations in *clr1*, *clr2*, or *clr3* clearly have a weaker effect at the *imr1R(NcoI)::ura4⁺* and *otr1R(SphI)::ura4⁺* insertion sites than the *clr4*, *rik1*, and *swi6* mutations. The *clr1-5*, *clr2-E22*, *swi6-115*, and *swi6Δ::his1⁺* mutations appear to have little or no effect on the *cnt1/TM1(NcoI)::ura4⁺* insertion site (Fig. 4).

Northern analyses (Fig. 5) show that in many cases the presence of a mutant locus leads to slight increases in the level of expression from the *cen1* inserted *ura4⁺* genes. However, certain mutations have their greatest effect on certain *ura4⁺* insertion sites. In strains with the *cnt1/TM1::ura4⁺* insertion, none of the mutations tested caused substantial derepression (expression of *ura4⁺* is up to a maximum of 0.2 of the minigene control). At the *imr1R(NcoI)::ura4⁺* and *otr1R(SphI)::ura4⁺* insertion sites, the *clr1*, *clr2*, *clr3*, and *swi6* mutations only result in partial derepression of the *ura4⁺* gene. In contrast, at both of these sites, the presence of the *clr4-S5* or *rik1-304* mutations almost abolishes repression so that the level of *ura4⁺* expression is elevated to between 0.85 and 0.95 of the minigene control. This suggests that there are distinct domains within *cen1* that are highly sensitive to the *clr4-S5* and *rik1-304* lesions and other domains, such as the central region of *cen1*, which are not (see Fig. 7, below).

These data indicate that the products of the *clr1⁺*, *clr2⁺*, *clr3⁺*, *clr4⁺*, *rik1⁺*, and *swi6⁺* genes all participate in the formation of structures that mediate gene repression at the silent mating-type loci, adjacent to telomeres and within centromeres. Mutations at two of these loci, *clr4*, and *rik1*, have the greatest effect on the repressive mechanisms but only at certain sites within the centromere. The products of the *clr4⁺* and *rik1⁺* genes must therefore play a critical role in the formation of a heterochromatin-like structure at fission yeast centromeres. As only three sites of *ura4⁺* insertion within *cen1* were tested in all mutant backgrounds, it is possible that the *clr1*, *clr2*, *clr3*, and *swi6* mutations cause greater derepression at other untested centromeric sites.

The clr4, rik1, and swi6 mutations reduce the fidelity of linear and circular chromosome segregation

It is possible that the repressed state within fission yeast centromeres is a manifestation of higher order structures required for the formation of a functional centromere. Because *clr1-5*, *clr2-E22*, *clr3-E36*, *clr4-S5*, *rik1-304*, *swi6-115*, and *swi6Δ::his1⁺* mutations can all affect transcriptional repression within *cen1*, these mutations may interfere with the structures formed at the centromere and thereby impair centromere function.

The fission yeast minichromosome Ch16 is a 530-kb derivative of chromosome III and is lost in ~0.2% of all cells (Niwa et al. 1989). When Ch16 is lost from cells, they form red rather than white colonies on limited adenine plates. If loss occurs in the first division of a single cell on such a plate, then half of the resulting colony will retain the minichromosome and form a white sector,

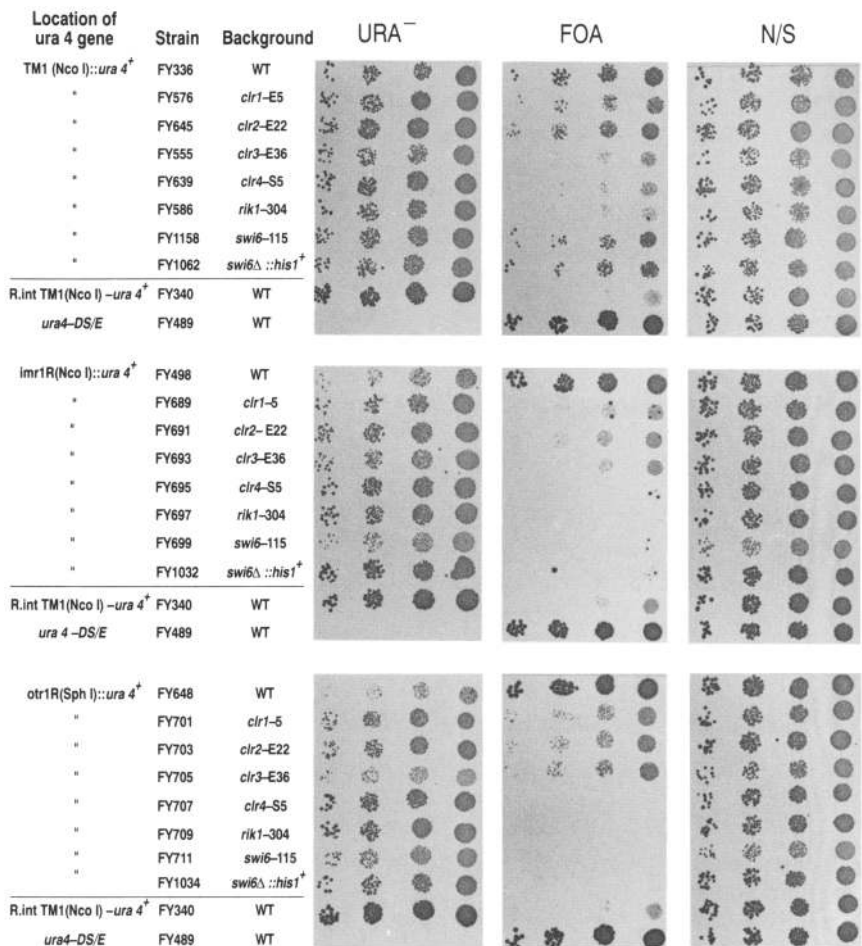


Figure 4. The effect of mutations at the *clr1*, *clr2*, *clr3*, *clr4*, *rik1*, and *swi6* loci on FOA resistance and uracil prototrophy at three sites of *ura4*⁺ insertion within *cen1*. Cultures with the *ura4*⁺ gene inserted at *cnt1*/TM1 (Nco I) (top), *imr1* (Nco I) (middle), and *otr1* (Sph I) (bottom) in wild-type and mutant backgrounds as shown were grown to 0.5×10^7 to 2.0×10^7 cells/ml in N/S medium. Serial dilutions (1:5) of each culture were spotted onto URA⁻, FOA, and N/S plates and incubated at 32°C for 3–4 days. The highest density spots contained 4×10^3 cells. FY340, which carries the *ura4*⁺ gene at a random site and grows as a fully *ura*⁺ strain, is included for comparison in each panel. FY489, which has no functional *ura4*⁺ gene, only the *ura4-DS/E* allele, is also included.

whereas the other half, with no minichromosome, will form a red sector. By scoring the frequency of half-sectored colonies, an accurate rate of chromosome loss per division can be calculated.

Strains bearing the minichromosome Ch16 and one of each of the mutations were constructed, and the rate of Ch16 loss compared with that in a wild-type background (Table 1A). The loss rate/division in wild type strains is not influenced by mating type and is similar to estimates published previously (Niwa et al. 1989). Strains bearing lesions at *clr1*, *clr2*, or *clr3*, which had weak effects on centromeric transcriptional repression, display rates of loss similar to wild type. In contrast, strains with the *clr4-S5* or *rik1-304* mutations missegregate the minichromosome in ~5% of cell divisions, almost a 100-fold increase over wild type. These same two loci have the greatest effect on transcriptional repression within centromeres (Fig. 5). Mutations at the *swi6* locus also affect chromosome segregation. In strains bearing *swi6-115* or *swi6Δ::his1*⁺, abnormal segregation is elevated 35- and 95-fold so that the minichromosome is lost in 1.8% and 4.9% of cell divisions, respectively.

The effect of these mutations on the segregation of normal chromosomes was also tested. Diploids homozygous for each mutation were forced by intragenic com-

plementation between the *ade6-210* (red) and *ade6-216* (pink) alleles. In the absence of selection for Ade⁺ cells, loss of a chromosome causes the diploid to revert rapidly to the haploid state forming red or pink sectors, allowing the rate of whole chromosome loss to be estimated. Table 1B demonstrates that the *clr4-S5*, *rik1-304*, and *swi6-115* mutations also cause elevated rates of loss of endogenous chromosomes.

Because the *clr1-5*, *clr2-E22*, *clr3-E36*, *clr4-S5*, *rik1-304*, and *swi6-115* mutations may affect gene repression at telomeres (i.e., little or no growth on FOA; Fig. 4C), it is possible that the elevated loss rate of the linear minichromosome Ch16 and whole chromosomes above was mediated through a defect in telomere function rather than changes in centromere structure and function. To test this possibility, the rate of loss of the 36-kb centromeric circular minichromosome CM3112 (Matsumoto et al. 1990) was measured in the presence and absence of all these mutations (Table 1C). Again the rate of chromosome loss is independent of mating type and *clr1-5*, *clr2-E22*, or *clr3-E36* have little or no effect on the CM3112 loss rate, which remains at between 1% and 2% of all divisions. The mis-segregation of this circular minichromosome occurs at such a high rate in strains bearing *clr4-S5*, *rik1-304*, and *swi6-115* mutations that an-

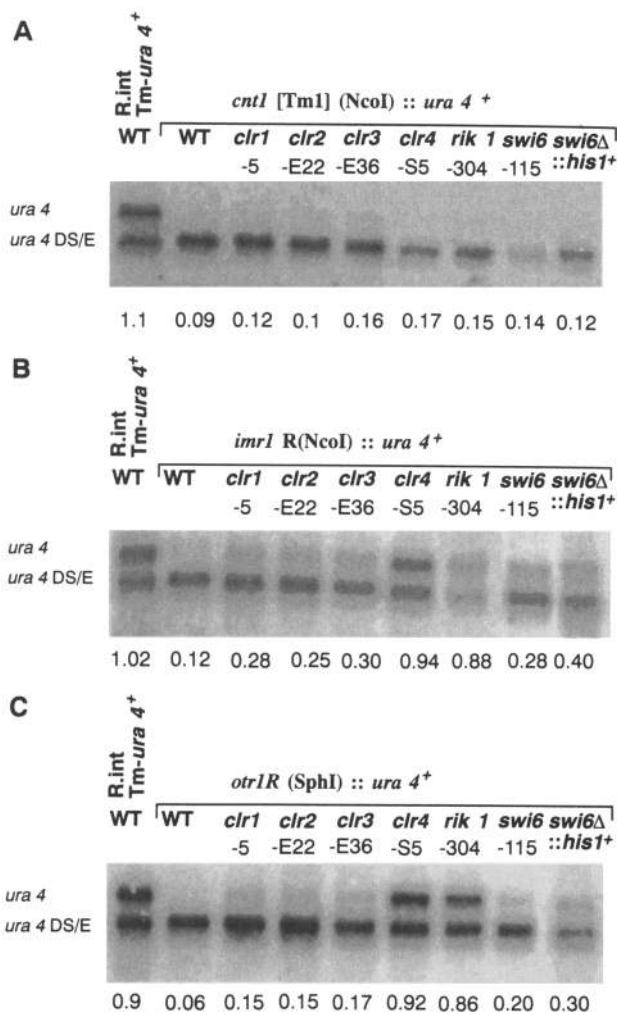


Figure 5. Mutations at *clr4* and *rik1* eliminate repression of *ura4*⁺ at distinct sites within *cen1*. Northern analyses of total RNA prepared from strains with *ura4*⁺ inserted at *cnt1*/Tm1 (A), *imr1* (NcoI) (B), and *otr1* (SphI) (C) in wild-type and mutant backgrounds as indicated. FY340, which expresses the *ura4*⁺ gene fully from a random site in the genome in the *ura4*-DS/E background, is included for comparison. The level of *ura4*⁺ mRNA produced relative to the *ura4*-DS/E control band was calculated from each PhosphorImage.

other method, more suited to estimating high loss rates, was employed (Kipling and Kearsy 1990). Table 1C shows that in strains with *clr4*-S5, *rik1*-304, or *swi6*-115 mutations the minichromosome CM3112 is lost in 18%, 17%, and 21% of divisions, respectively. This dramatic difference in the stability of CM3112 in wild-type versus *clr4*-S5, *rik1*-304, and *swi6*-115 backgrounds is illustrated in Figure 6. In *S. pombe*, acentric minichromosomes or *ars* containing plasmids are, in general, lost in 20–50% of cell divisions (Heyer et al. 1986; Matsumoto et al. 1990). Therefore, these results demonstrate that mitotic centromere function of the already compromised circular minichromosome CM3112 is almost completely obliterated in *clr4*-S5, *rik1*-304, and *swi6*-115 back-

grounds. This implies that the factors encoded by these genes are essential for the function of this minimal centromere.

Discussion

A zone of repression covering the centromeric domain

Transcription of the *ura4*⁺ gene is repressed at all 11 sites tested within the domain occupied by fission yeast *cen1*, as demarcated by the large inverted repeat surrounding the central region. At two sites outside this domain, the *ura4*⁺ gene is not repressed (Figs. 1 and 2). These two sites are 0.9 kb (*Xho*I) and 1.2 kb (*Hpa*I) outside the large inverted repeat as defined by Takahashi et

Table 1. Effect of *clr1*, *clr2*, *clr3*, *clr4*, *rik1*, and *swi6* mutations on the fidelity of chromosome transmission

A. The 530-kb linear minichromosome Ch16			
Loss rate			
Strain	Background	per division	percent divisions
FY521	WT h ⁺	4.4 × 10 ⁻⁴	0.044
FY721	WT h ⁻	5.8 × 10 ⁻⁴	0.058
FY723	<i>clr1</i> -5	1.7 × 10 ⁻³	0.17
FY725	<i>clr2</i> -E22	1.9 × 10 ⁻³	0.19
FY727	<i>clr3</i> -E36	1.1 × 10 ⁻³	0.11
FY729	<i>clr4</i> -S5	4.9 × 10 ⁻²	4.90
FY731	<i>rik1</i> -304	4.8 × 10 ⁻²	4.8
FY733	<i>swi6</i> -115	1.8 × 10 ⁻²	1.8
FY1036	<i>swi6</i> Δ :: <i>his1</i> ⁺	4.9 × 10 ⁻²	4.9

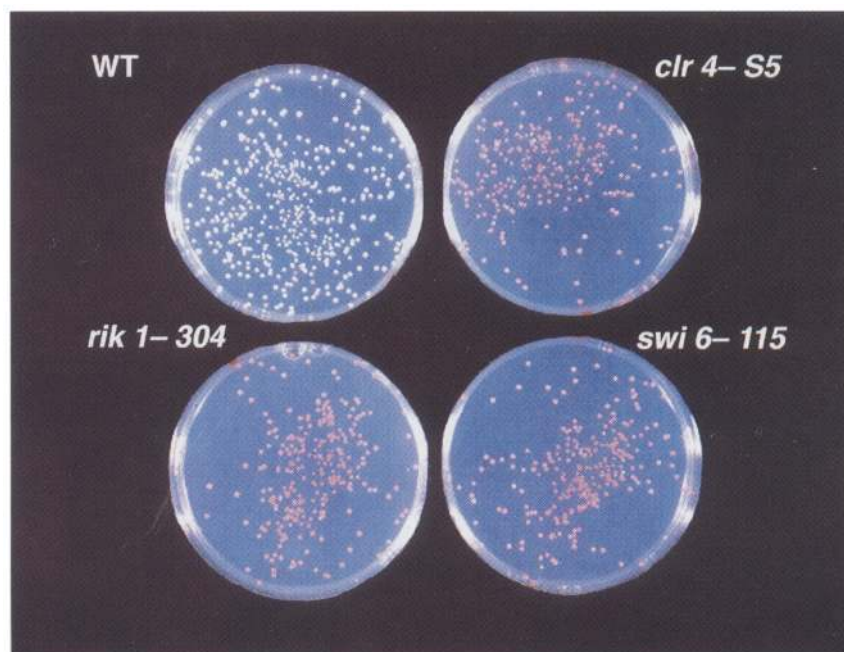
B. Whole chromosomes monitored by breakdown of diploids			
Loss rate			
Strain	Background	per division	percent divisions
FY1100	WT	<1 × 10 ⁻³	<0.1 ^a
FY1102	<i>clr1</i> -5	<1 × 10 ⁻³	<0.1 ^a
FY1104	<i>clr2</i> -E22	<1 × 10 ⁻³	<0.1 ^a
FY1106	<i>clr3</i> -E36	<1 × 10 ⁻³	<0.1 ^a
FY1108	<i>clr4</i> -S5	4.7 × 10 ⁻²	4.7 ^a
FY1110	<i>rik1</i> -304	3.2 × 10 ⁻²	3.2 ^a
FY1112	<i>swi6</i> -115	2.4 × 10 ⁻²	2.4 ^a

C. The 30-kb circular minichromosome CM3112

Loss rate			
Strain	Background	per division	percent divisions
FY759	WT h ⁺	1.1 × 10 ⁻²	1.1
FY865	WT h ⁻	9.0 × 10 ⁻³	0.9
FY853	<i>clr1</i> -5	1.5 × 10 ⁻²	1.2
FY787	<i>clr2</i> -E22	7.9 × 10 ⁻³	0.8
FY790	<i>clr3</i> -E36	1.7 × 10 ⁻²	1.7
FY856	<i>clr4</i> -S5	1.8 × 10 ⁻¹	18.0 ^a
FY859	<i>rik1</i> -304	1.7 × 10 ⁻¹	17.0 ^a
FY862	<i>swi6</i> -115	2.1 × 10 ⁻¹	21.0 ^a

^aThe loss rate was determined by the method of Kipling and Kearsy (1990).

Figure 6. Mutations at *clr4*, *rik1*, and *swi6* disrupt segregation of a circular minichromosome. Wild-type (FY759), *clr4-S5* (FY856), *rik1-304* (FY859), and *swi6-115* (FY862) colonies containing the circular minichromosome CM3112 were picked from plates selecting for the minichromosome (*Ade*⁻), resuspended in N/S medium, and plated onto YE+0.15A plates. Colonies retaining the minichromosome are white; those without it are red. Minichromosome loss during colony outgrowth results in white colonies with red sectors. Little or no white sectors are visible in the strains bearing either the *rik1-304*, *clr4-S5*, or *swi6-115* lesions, indicating that centromere function is severely disrupted in the presence any of these mutations.



al. (1992), although other data (Steiner et al. 1993; R. Allshire and G. Cranston, unpubl.) suggest that this inverted repeat extends at least as far as the *HpaI* site (Fig. 2A). At the *BglII* insertion site at the end of the *otr* region, *ura4*⁺ transcription is repressed. The fact that at a site only 0.9 kb (*XhoI*, FY937) further away little repression is observed indicates that the centromeric zone of repression must terminate abruptly within this 0.9-kb region. It is conceivable that the 0.9-kb region contains a specific sequence that acts as a barrier to the formation of repressive structures outside this region. It has been postulated that specific terminators are required to halt the assembly of heterochromatin along a chromosome (see Eissenberg 1989). Specific DNA fragments have been identified that, in *Drosophila*, insulate genes from position effects (Kellum and Schedl 1991; Chung et al. 1993). The 0.9-kb *cen1* region may have a similar role in insulating neighboring genes from centromeric repression. Alternatively, the large inverted repeat within the centromere may form a higher order structure, such as a hairpin (see Fig. 7c), which mediates repression. In this case, the *HpaI* and *XhoI* sites would lie at the base of this structure and might be less prone to repression.

Repression, unusual centromeric chromatin, and repeats

The central domain of fission yeast centromeres forms unusual chromatin (Polizzi and Clarke 1991; Takahashi et al. 1992), which we have shown influences the chromatin structure of the *ura4*⁺ gene when placed in the center of *cen1* or *cen2* (Allshire et al. 1994). We proposed that this unusual chromatin was causally related to the repression of *ura4*⁺ observed at these sites. It was therefore surprising to find that the *ura4*⁺ gene is also re-

pressed in the outer domains of *cen1* where the DNA is packaged into regular nucleosomes. This suggests that either different mechanisms of repression operate in these different domains or that the alteration in *ura4*⁺ chromatin structure within *cen1* and *cen2* does not mediate repression.

Clarke et al. (1993) have observed that all functional centromere constructs assemble unusual chromatin in the central domain, whereas nonfunctional constructs do not. This suggests a link between specialized chromatin structure and centromere function. It is also possible that a higher order structure, for example a hairpin configuration (such as that proposed by Takahashi et al. 1992; Clarke et al. 1993; see Fig. 7c), is required to mediate both centromeric repression and centromere function. Recent observations in *Drosophila* indicate that tandem or inverted repeats of a minigene have a propensity to interact and mediate their own repression. In some configurations this repression is sensitive to common suppressors of variegating position effects such as mutations in the *Suvar(2)5* gene encoding HP1 (Dorer and Henikoff 1994). It has been proposed that repression is brought about by the pairing of copies of the minigene so as to exclude transcription factors. Other phenomena related to PEV, such as *trans*-sensing, are also thought to rely on somatic pairing (Henikoff 1994). It is therefore intriguing that, apart from containing large inverted repeats of 18 kb or more, all fission yeast centromeres cluster together at the nuclear periphery in interphase (Funabiki et al. 1993) and that genes are also repressed at fission yeast telomeres (Nimmo et al. 1994) which also form aggregates at the nuclear periphery (Funabiki et al. 1993). Credence to the idea that a higher order structure is required for fission yeast centromere function comes from the observation that certain minichromosome con-

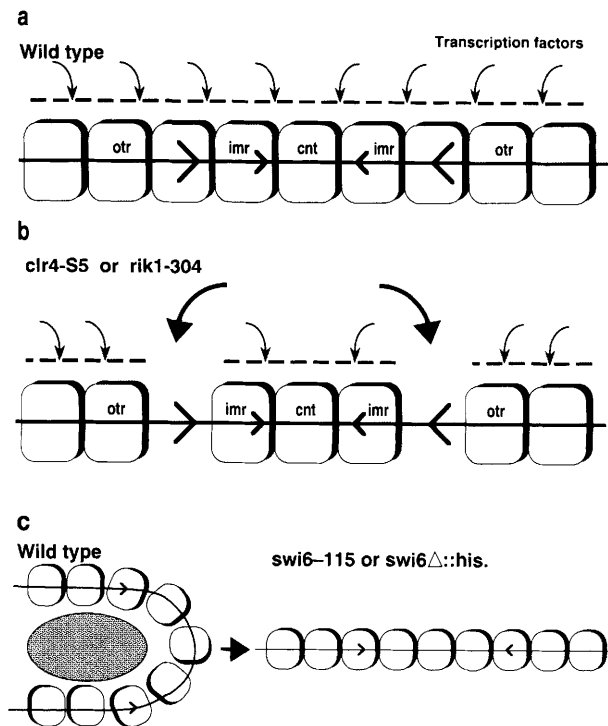


Figure 7. Schematic representation of the structure of *cen1* and the effect of *clr4*, *rik1*, and *swi6* mutations on silencing and centromere function. (a) The region occupied by *cen1* is coated with a nonuniform heterochromatin-like structure, different forms of which are specific to certain domains within the centromere. In wild-type strains, this heterochromatin-like structure restricts the accessibility of the centromere to transcription factors (small arrows). The whole centromere may be folded into a higher order structure as in c. (b) In strains carrying *clr4-S5* or *rik1-304* mutations, transcription in the central domain (*cnt1*) remains limited (as shown by Northern analyses; Fig. 5) but the domain encompassing at least a 1.3-kb region spanning the *otr1* and *imr1* border becomes very accessible to transcription factors (large arrows). The *clr1*, *clr2*, *clr3*, *clr4*, and *rik1* mutations may cause a relaxation in the central domain (see Fig. 4), but the *swi6* mutations have no phenotype with respect to silencing in this region. All six mutations increase accessibility in the *imr1/otr1* region tested, but only the *clr4* and *rik1* mutations abolish this repression. (c) In wild-type cells, the product of the *swi6*⁺ gene may be required alone or in a complex (large shaded oval) to facilitate the formation of a higher order structure, such as a hairpin (Takahashi et al. 1992; Clarke et al. 1993), by interacting with components of the heterochromatin-like structure. Mutations at the *swi6* locus would interfere with the formation of this structure, disrupting centromere function but not completely abolishing transcriptional repression. Mutations such as *clr4-S5* and *rik1-304*, which disrupt this heterochromatin-like structure, would also interfere with the formation of this secondary structure and centromere function.

structs are apparently regulated in an epigenetic manner so that a functional centromere is only formed in some lineages (Clarke et al. 1993; Steiner and Clarke 1994). Such constructs may have difficulty in folding into the correct conformation to form a functional centromere.

Transcriptional repression linked to centromere function in fission yeast

We have shown that mutations at *clr4* and *rik1* derepress the *ura4*⁺ gene at certain sites within fission yeast *cen1* much more than those at *clr1*, *clr2*, *clr3*, or *swi6*. All of these mutations have minimal effects on the expression of the *ura4*⁺ gene at telomeres and no effect on expression of the *ura4*⁺ gene from a random integration site. Strains bearing either *clr4* or *rik1* mutations also display highly elevated rates of chromosome loss. In contrast, the *clr1*, *clr2*, and *clr3* mutations have a negligible effect on chromosome segregation. This strongly suggests that the zone of repression formed within fission yeast centromeres has an integral role in the formation of fully functional centromeres. In Figure 7a this zone of repression is depicted as the centromeric DNA coated with a heterochromatin-like structure that is refractory to transcription factors. This centromeric zone of repression appears to be divided into separate domains. The central region remains resistant to transcription in strains bearing any of the mutations tested. However, in the presence of the *clr4-S5* or *rik1-304* mutation, the flanking domains are released and become accessible for transcription (Fig. 7b). It is envisaged that this heterochromatin-like structure is required, directly or indirectly, to either maintain the attachment of sister chromatids during mitosis up until the onset of anaphase or form the foundations for the assembly of a functional kinetochore and its attachment to the microtubules emanating from the spindle pole body.

Strains bearing mutations at the *swi6* locus also exhibit high rates of chromosome loss even though they have weaker effects on repression at the three centromeric sites tested. It is possible that these *swi6* mutations cause complete derepression at other untested regions of the centromere, although complete derepression per se is not necessarily a prerequisite for defective centromere function. Alternatively, the *swi6* protein might be involved in facilitating the formation of a higher order structure on the underlying heterochromatin but is not directly involved in mediating transcriptional repression at centromeres (Fig. 7c). To explain the effects of the *swi6-115* mutation on the directionality of mating-type switching, it has been proposed previously that the *swi6* product promotes intrachromosomal folding of the silent mating-type loci onto *mat1* (Thon and Klar 1993). In addition to *clr4*⁺, *rik1*⁺, and *swi6*⁺, it is conceivable that the products of the *clr1*⁺, *clr2*⁺, and *clr3*⁺ genes have an auxiliary role in the formation of centromeric heterochromatin, but they are not critical for centromere function.

Heterochromatin and centromere function in other organisms

In many eukaryotes, the centromeric region is associated with arrays of repetitive DNA such as alphoid satellite in humans, minor satellite in mouse, and simple and complex satellite DNA in *Drosophila* (Miklos and Cotsell

1990; Rattner 1991; Tyler-Smith and Willard 1993). These regions are normally packaged as heterochromatin and therefore tend to be late replicating and suppressed for recombination and to show frequent associations with the nuclear periphery (see introductory section). Although the exact role of these heterochromatic regions in centromere function and kinetochore assembly remains to be elucidated, several studies indicate that they contribute to centromere function. At human centromeres, although CENP-B is associated with both active and inactive centromeres, alphoid repeats associated with CENP-B underlie the kinetochore (Cooke et al. 1990) and injection of dividing cells with predominantly anti-CENP-B antibodies leads to some disruption of kinetochore structure, which may be the result of alteration in the compaction of the underlying chromatin (Bernat et al. 1991). Alphoid repeats inserted at noncentromeric sites may display some aspects of centromere function (Haaf et al. 1992; Larin et al. 1994). In *Drosophila* it is known that certain alleles of *Suvar(3)6* (encoding protein phosphatase 1), which suppresses variegation of *white* adjacent to heterochromatin, can result in abnormal chromosome segregation (Baska et al. 1993). Again in *Drosophila*, a marker chromosome responds to suppressors of variegating position effects, so that in genetic backgrounds where there is less repression of reporter genes, and presumably less heterochromatin, this chromosome is less stable. Analyses of aberrant mitotic configurations in these flies suggested that the nondisjunction events resulted from premature sister chromatid separation (Wines and Henikoff 1992). This implies that the amount of DNA packaged as heterochromatin within a centromeric domain directly influences the functionality of that centromere.

Of the three genes that we have shown to disrupt centromere function (*clr4*⁺, *rik1*⁺, and *swi6*⁺), only the *swi6*⁺ gene has been cloned and sequenced. It is intriguing that *swi6*⁺ encodes a protein containing a chromodomain and plays a role in transcriptional silencing and perhaps in the formation of a folded structure at the *mat* loci (Thon and Klar 1993; Lorentz et al. 1994). Other chromodomain-containing proteins, such as HP1, are known to be associated with centromeric heterochromatin (see introductory section). Mutations in the *Drosophila* chromodomain protein HP1 [*Suvar(2)5*] alleviate repression of variegating genes, whereas increased dosage of the wild-type gene enhances this repression (Eisenberg et al. 1992). Recently, it has been observed that aberrant chromosome segregation occurs in *Drosophila* embryos homozygous for HP1 mutations. These embryos contain a high frequency of nuclei with lagging chromosomes and anaphase/telophase bridges (R. Kellum and B. Alberts, pers. comm.). Clearly, this also implies that normal chromosome segregation is dependent on the integrity of centromeric heterochromatin.

Concluding remarks

Further analyses of the *clr4*⁺, *rik1*⁺, and *swi6*⁺ genes and their products should lead to a more complete un-

derstanding of their role in centromere function. At present, the product of *swi6*⁺ is a good candidate for a component of a heterochromatin-like structure at centromeres and at other sites in fission yeast. The products of *clr4*⁺ and *rik1*⁺ could also be components of heterochromatin-like structures or may play a role in the regulation of such structures. Our analyses indicate that the *clr4*⁺, *rik1*⁺, and *swi6*⁺ genes have important roles at both centromeres and the silent mating-type loci, whereas the *clr1*⁺, *clr2*⁺, and *clr3*⁺ genes have a less critical role at the former. Further genetic and molecular analyses may reveal other factors that only play a critical role in centromeric transcriptional repression and centromere function. Such factors might include DNA-binding proteins that interact specifically with certain DNA sequences at centromeres. Alternatively, other centromere-specific non-DNA-binding factors, required for the assembly of a functional kinetochore, may be identified. Such factors might simultaneously associate with the products of the *clr4*⁺, *rik1*⁺, or *swi6*⁺ genes to form heterochromatin at fission yeast centromeres that promotes the assembly of a functional kinetochore.

Materials and methods

Plasmid constructions

p13-18dg1/glu

Oligonucleotides were designed to amplify a region between *dg1/K''* (CCATCCGCAGTTGGGAGTAC), and the 3' end of the *glu* tRNA in *imr1/B'*. *Bam*HI sites were added during the PCR reaction. A product of ~2.3 kb was gel-purified, digested with *Bam*HI, and cloned in *puc13-18*. To eliminate certain sites, the 2.3-kb insert was recloned in the *Bam*HI site of *puc18-13* to give *puc18-13dg1/glu*.

p13-18dg1/glu(SphI)-ura4 The *ura4*⁺ gene on a 1.75-kb *SphI* fragment from *pSpHura4* was cloned in both orientations into the *SphI* site in the *dg1* region of *p13-18dg1/glu*.

p13-18dg1/glu(NcoI)-ura4 The *ura4*⁺ gene on a 1.75-kb *Hind*III fragment was treated with Klenow and inserted in both orientations into the filled-in *NcoI* site of *p13-18dg1/glu*.

pGEMimr1LNcoI/SphI(aeHindIII)-ura4 The 1.45-kb *NcoI-SphI* fragment from *pCC1R* (contains the right-side 6-kb *NcoI* fragment from the middle of *cen1*) was subcloned into *pGEM7* (Promega). The *ura4*⁺ gene on a 1.75-kb *Hind*III fragment was inserted into the *Hind*III site between the alanine (a) and glutamic acid (e) tRNA genes.

pBSimr1RClaI/EcoRI(iHindIII)-ura4 The 1.81-kb *ClaI-EcoRI* fragment from *pCC1R* was cloned into *pBS/SK*. The *ura4*⁺ gene on a 1.75-kb *Hind*III fragment was inserted into the *Hind*III site close to the isoleucine (i) tRNA gene.

pPhe-otr1, *pPhe-otr1(XhoI)-ura4* and *pPhe-otr1(HpaI)-ura4* Oligonucleotides were designed to amplify the region between the Phe tRNA CCCAACTACACCATGCGACTTC (flanking the left side of *cen1*; Takahashi et al. 1992) and the end of *otr1* CAGTTGACTAGGATTTGTTTG (*dh1a/K'*). Terminal *Bam*HI sites were added during PCR. The 1.8-kb *Bam*HI PCR product was cloned in *puc18/13*. *XhoI* and *HpaI* cut 0.9 and 1.2 kb from the end of *otr1*, respectively. *pPhe-otr1* was cleaved with *XhoI* or *HpaI* and treated with Klenow, and the filled-in 1.75-kb

ura4⁺ HindIII fragment was inserted at both sites generating pPhe-*otr1*(XhoI)-*ura4* and pPhe-*otr1*(HpaI)-*ura4*.

pPhe-otr1/dh1XhoI/SphI(BglII)-ura4 Oligonucleotides were designed to amplify the region between the Phe tRNA (same oligo as above) and part of *dh1a/K'* CCAGCTTTATGCCAAAACATGCATG. The 2.2-kb PCR product was digested with XhoI and SphI, and the 1.4-kb fragment was cloned in pGEM7. The *ura4⁺* gene on a 1.75-kb BamHI fragment from puc13/18-*ura4* was cloned in both orientations (oriI and oriII) into the BglII site at the end of *dh1a/K'*.

puc21otr1-dhNdeI/BglII(HindIII)-ura4 Oligonucleotides were designed to generate a 1.15-kb PCR product spanning the NdeI-BglII region of *dh1a/K'* of *cen1* (GAACATTTCTCAGAT-TAAAAAGTC and GCCATGTAATCTAAAACCTTACCG). The product was digested with NdeI and BglII, and the 1.08-kb fragment was inserted into puc21. The *ura4⁺* gene on a 1.75-kb HindIII fragment was cloned in both orientations (oriI and oriII) into the HindIII site located in the insert.

potr1-dg1a/K''(HindIII)-ura4 A 2.22-kb PCR product generated with oligonucleotides CAGGGCATGCTTAGCAAGTAC and GGCATAGCGATGATAGTTCTA spanning the Asp718 and SphI sites within *dg1a/K''* of *cen1* was cut with these enzymes and cloned in puc21. The *ura4⁺* gene on a 1.75-kb HindIII fragment was cloned in the HindIII site located in the insert.

S. pombe media

Media were essentially as described by Moreno et al. (1991) and in Allshire et al. (1994). For chromosome loss tests, YE plates were supplemented with 0.15 the normal amount of adenine (YE + 0.15A, 12 mg/liter). Comparative plating and serial dilution experiments were performed as described previously (Allshire et al. 1994; Nimmo et al. 1994).

Strain construction

For transformation, a simplified version of the lithium acetate pH 4.9 procedure was used (Moreno et al. 1991). The genotype of all strains used is presented in Table 2. FY489 contains a 280-bp deletion in the *ura4⁺* gene at the *ura4* locus and was derived by crossing FY290 with FY200 (Allshire et al. 1994).

To insert the *ura4⁺* gene at sites within *cen1*, the same general procedure was followed in each case. A linear DNA fragment with the region of interest disrupted by the *ura4⁺* gene was released from various plasmids, gel-purified, and used to transform the strain SP813.

Ura⁺ transformants (200–2000) were then subjected to a simple stability test by streaking for single colonies on FOA plates. Single colonies were picked from each original colony that grew in the presence of FOA and again restreaked on FOA plates. These two rounds of streaking for FOA^R colonies ensured the loss of episomal forms. Colonies that grew were then streaked onto URA⁻ plates to identify cells retaining the *ura4⁺* gene. DNA analyses confirmed the presence of the *ura4⁺* gene at the desired site within the centromere.

Within the *imr1* and *cnt1* regions, digestion with ClaI allowed insertions into the left and right sides of the inverted structure to be distinguished. Digestion with HpaI allowed insertion within the left and right Phe-*dh1a/K'* regions to be distinguished. The starting strain, SP813, carries a complete deletion of the *ura4⁺* gene (*ura4-D18*). After confirming that transformants had an insertion at the correct site on the left or right side of *cen1*, all were crossed with FY489 to introduce the truncated allele of *ura4* (*ura4-DS/E*), allowing quantification of

ura4⁺ RNA levels produced from each site. Pulse-field gel electrophoresis after SalI digestion of large DNA prepared in agarose plugs from strains with *ura4⁺* insertions within *cen1* demonstrated that no gross structural alterations had occurred. After hybridization with a *ura4⁺* probe, the expected SalI fragment of ~65 kb containing the whole *cen1* region could be detected in each strain (data not shown). Other digests also indicated that the normal structure of *cen1* was maintained.

FY336 and FY340 were described by Allshire et al. (1994). FY520 and FY521 were described by Nimmo et al. (1994). FY597 was derived from a cross between PG9 (Thon and Klar 1992) and FY489. FY1028, the *swi6⁺* gene, was replaced with *his1⁺* (Iain Hagan, University of Manchester, UK), resulting in *swi6Δ::his1⁺*, similar to that described previously (Lorentz et al. 1994).

The *clr1-5*, *clr2-E22*, *clr3-E36*, *clr4-S5*, *rik1-304*, and *swi6-115* mutations were followed in crosses by iodine staining and visual examination of cells by phase-contrast microscopy for those undergoing haploid meiosis (Thon and Klar 1992; Ekwall and Ruusala 1994; Lorentz et al. 1994). After crossing with FY489, the strains FY530, FY602, FY637, FY514, FY512, FY528, and FY1028 were generated, and these strains that bear the *clr1-5*, *clr2-E22*, *clr3-E36*, *clr4-S5*, *rik1-304*, *swi6-115*, or *swi6Δ::his1⁺* mutations and the *ura4-DS/E* allele were crossed with FY336, FY498, FY648, FY527, FY520, FY597, FY340, FY521, and FY757, generating a series of isogenic strains (see Table 2).

Mitotic chromosome stability assays

Cells (500–1000) from Ade⁺ colonies were plated on YE + 0.15 adenine plates and incubated at 32°C for 3–5 days followed by 2–3 days at 4°C to allow the red color to deepen. The number of colonies with a red sector covering at least half of the colony was counted. The number of chromosome loss events per division is the number of these half-sectored colonies divided by the total number of white colonies plus half-sectored colonies. The rate of loss of the circular minichromosome, CM3112, was too high to use the above method. Another method was employed (Kipling and Kearsley 1990). Briefly, an Ade⁺ colony was picked, resuspended in a small volume of medium, and the cell density was measured. Cells (500–1000) were plated on Ade⁻ plates to estimate the proportion of cells in the colony containing the minichromosome. Cells (1 × 10⁴) from the same colony were grown in the absence of selection (Ade⁺ plates) for 15–20 generations, after which time the proportion of cells retaining the minichromosome was again estimated by plating on Ade⁻ plates at 32°C. The rate of chromosome loss per division was estimated using the formula: loss rate = 1 - (F/I)^{1/N}, where F is the final percentage of cells bearing the minichromosome, I is the initial percentage of cells carrying the minichromosome, and N is the number of generations between I and F (Kipling and Kearsley 1990).

DNA preparation, digestion, and analyses

DNA was extracted essentially as described in Moreno et al. (1991). High-molecular-weight DNA in agarose blocks for analysis by PFGE was prepared as described in Allshire (1992). DNA was digested according to the manufacturer's recommended conditions and analyzed by electrophoresis on 0.7–1.5% agarose gels in 0.5 × TAE buffer. For PFGE analyses, samples were loaded on a 1% agarose gel in 0.5 × TAE buffer. To separate all three centromeric SalI fragments, the gel was run on a Biorad Cheffil system for 22 hr at 200 V with a pulse time starting at 2 sec and ending at 20 sec. DNA was transferred and hybridiza-

Table 2. *S. pombe* strains used in this study

Strain	Position and <i>ura4</i> gene	Genotype	
972	wild-type	<i>h</i> ⁻	
SP813	deleted	<i>h</i> ⁺	<i>leu1-32 ade6-210, ura4-D18</i>
FY489	<i>ura4-DS/E</i>	<i>h</i> ⁻	<i>leu1-32, ade6-210, ura4-DS/E</i>
FY340	TM1(<i>NcoI</i>)- <i>ura4</i> Random int.	<i>h</i> ⁺	<i>leu1-32, ade6-210, leu4-DS/E</i>
FY496	<i>imr1L(NcoI)::ura4 oriI</i>	<i>h</i> ⁺	<i>leu1-32, ade6-210, ura4-DS/E</i>
FY501	<i>imr1L(NcoI)::ura4 oriII</i>	<i>h</i> ⁺	<i>leu1-32, ade6-210, ura4-DS/E</i>
FY502	<i>imr1R(NcoI)::ura4 oriII</i>	<i>h</i> ⁺	<i>leu1-32, ade6-210, ura4-DS/E</i>
FY524	<i>imr1R(aeHindIII)::ura4</i>	<i>h</i> ⁺	<i>leu1-32, ade6-210, ura4-DS/E</i>
FY525	<i>imr1L(aeHindIII)::ura4</i>	<i>h</i> ⁺	<i>leu1-32, ade6-210, ura4-DS/E</i>
FY527	<i>imr1R(iHindIII)::ura4</i>	<i>h</i> ⁺	<i>leu1-32, ade6-210, ura4-DS/E</i>
FY534	<i>imr1L(iHindIII)::ura4</i>	<i>h</i> ⁺	<i>leu1-32, ade6-210, ura4-DS/E</i>
FY941	Phe- <i>otr1L(HpaI)::ura4</i>	<i>h</i> ⁺	<i>leu1-32, ade6-210, ura4-DS/E</i>
FY937	Phe- <i>otr1L(XhoI)::ura4</i>	<i>h</i> ⁺	<i>leu1-32, ade6-210, ura4-DS/E</i>
FY939	<i>otr1L(dh/BgIII)::ura4 oriII</i>	<i>h</i> ⁺	<i>leu1-32, ade6-210, ura4-DS/E</i>
FY988	<i>otr1L(dh/BgIII)::ura4 oriI</i>	<i>h</i> ⁺	<i>leu1-32, ade6-210, ura4-DS/E</i>
FY965	<i>otr1L(dh/HindIII)::ura4 oriI</i>	<i>h</i> ⁺	<i>leu1-32, ade6-210, ura4-DS/E</i>
FY967	<i>otr1L(dh/HindIII)::ura4 oriII</i>	<i>h</i> ⁺	<i>leu1-32, ade6-210, ura4-DS/E</i>
FY986	<i>otr1L(dg1a/HindIII)::ura4 oriII</i>	<i>h</i> ⁺	<i>leu1-32, ade6-210, ura4-DS/E</i>
FY336	<i>cnt1/TM1(NcoI)::ura4</i>	<i>h</i> ⁺	<i>leu1-32, ade6-210, ura4-DS/E</i>
FY576	<i>cnt1/TM1(NcoI)::ura4</i>	<i>h</i> ^A	<i>leu1-32, ade6-210, ura4-DS/E clr1-5</i>
FY645	<i>cnt1/TM1(NcoI)::ura4</i>	<i>h</i> ^A	<i>leu1-32, ade6-210, ura4-DS/E clr2-E22</i>
FY555	<i>cnt1/TM1(NcoI)::ura4</i>	<i>h</i> ^A	<i>leu1-32, ade6-210, ura4-DS/E clr3-E36</i>
FY639	<i>cnt1/TM1(NcoI)::ura4</i>	<i>h</i> ^A	<i>leu1-32, ade6-210, ura4-DS/E clr4-S5</i>
FY586	<i>cnt1/TM1(NcoI)::ura4</i>	<i>h</i> ^A	<i>leu1-32, ade6-210, ura4-DS/E rik1-304</i>
FY1158	<i>cnt1/TM1(NcoI)::ura4</i>	<i>h</i> ^A	<i>leu1-32, ade6-210, ura4-DS/E swi6-115</i>
FY1062	<i>cnt1/TM1(NcoI)::ura4</i>	<i>h</i> ^A	<i>leu1-32, ade6-210, ura4-DS/E his1-102 swi6Δ::his1⁺</i>
FY498	<i>imr1R(NcoI)::ura4 oriI</i>	<i>h</i> ⁺	<i>leu1-32, ade6-210, ura4-DS/E</i>
FY689	<i>imr1R(NcoI)::ura4 oriI</i>	<i>h</i> ^A	<i>leu1-32, ade6-210, ura4-DS/E clr1-5</i>
FY691	<i>imr1R(NcoI)::ura4 oriI</i>	<i>h</i> ^A	<i>leu1-32, ade6-210, ura4-DS/E clr2-E22</i>
FY693	<i>imr1R(NcoI)::ura4 oriI</i>	<i>h</i> ^A	<i>leu1-32, ade6-210, ura4-DS/E clr3-E36</i>
FY695	<i>imr1R(NcoI)::ura4 oriI</i>	<i>h</i> ^A	<i>leu1-32, ade6-210, ura4-DS/E clr4-S5</i>
FY697	<i>imr1R(NcoI)::ura4 oriI</i>	<i>h</i> ^A	<i>leu1-32, ade6-210, ura4-DS/E rik1-304</i>
FY699	<i>imr1R(NcoI)::ura4 oriI</i>	<i>h</i> ^A	<i>leu1-32, ade6-210, ura4-DS/E swi6-115</i>
FY1032	<i>imr1R(NcoI)::ura4 oriI</i>	<i>h</i> ^A	<i>leu1-32, ade6-210, ura4-DS/E his1-102 swi6Δ::his1⁺</i>
FY648	<i>otr1R(SphI)::ura4</i>	<i>h</i> ⁺	<i>leu1-32, ade6-210, ura4-DS/E his1-102 swi6Δ::his1⁺</i>
FY701	<i>otr1R(SphI)::ura4</i>	<i>h</i> ^A	<i>leu1-32, ade6-210, ura4-DS/E clr1-5</i>
FY703	<i>otr1R(SphI)::ura4</i>	<i>h</i> ^A	<i>leu1-32, ade6-210, ura4-DS/E clr2-E22</i>
FY705	<i>otr1R(SphI)::ura4</i>	<i>h</i> ^A	<i>leu1-32, ade6-210, ura4-DS/E clr3-E36</i>
FY707	<i>otr1R(SphI)::ura4</i>	<i>h</i> ^A	<i>leu1-32, ade6-210, ura4-DS/E clr4-S5</i>
FY709	<i>otr1R(SphI)::ura4</i>	<i>h</i> ^A	<i>leu1-32, ade6-210, ura4-DS/E rik1-304</i>
FY711	<i>otr1R(SphI)::ura4</i>	<i>h</i> ^A	<i>leu1-32, ade6-210, ura4-DS/E swi6-115</i>
FY1034	<i>otr1R(SphI)::ura4</i>	<i>h</i> ^A	<i>leu1-32, ade6-210, ura4-DS/E his1-102 swi6Δ::his1⁺</i>
FY597	<i>mat3-M(EcoRV)::ura4</i>	<i>h</i> ⁹⁰	<i>leu1-32, ade6-210, ura4-DS/E</i>
FY624	<i>mat3-M(EcoRV)::ura4</i>	<i>h</i> ^A	<i>leu1-32, ade6-210, ura4-DS/E clr1-5</i>
FY633	<i>mat3-M(EcoRV)::ura4</i>	<i>h</i> ^A	<i>leu1-32, ade6-210, ura4-DS/E clr2-E22</i>
FY627	<i>mat3-M(EcoRV)::ura4</i>	<i>h</i> ^A	<i>leu1-32, ade6-210, ura4-DS/E clr3-E36</i>
FY629	<i>mat3-M(EcoRV)::ura4</i>	<i>h</i> ^A	<i>leu1-32, ade6-210, ura4-DS/E clr4-S5</i>
FY631	<i>mat3-M(EcoRV)::ura4</i>	<i>h</i> ^A	<i>leu1-32, ade6-210, ura4-DS/E rik1-304</i>
FY622	<i>mat3-M(EcoRV)::ura4</i>	<i>h</i> ^A	<i>leu1-32, ade6-210, ura4-DS/E swi6-115</i>
FY520	Ch16 m23:: <i>ura4</i> -TEL[72]	<i>h</i> ⁺	<i>leu1-32, ade6-210, ura4-DS/E (Ch16 ade6-216)</i>
FY612	Ch16 m23:: <i>ura4</i> -TEL[72]	<i>h</i> ^A	<i>leu1-32, ade6-210, ura4-DS/E (Ch16 ade6-216) clr1-5</i>
FY736	Ch16 m23:: <i>ura4</i> -TEL[72]	<i>h</i> ^A	<i>leu1-32, ade6-210, ura4-DS/E (Ch16 ade6-216) clr2-E22</i>
FY613	Ch16 m23:: <i>ura4</i> -TEL[72]	<i>h</i> ^A	<i>leu1-32, ade6-210, ura4-DS/E (Ch16 ade6-216) clr3-E36</i>
FY738	Ch16 m23:: <i>ura4</i> -TEL[72]	<i>h</i> ^A	<i>leu1-32, ade6-210, ura4-DS/E (Ch16 ade6-216) clr4-S5</i>
FY898	Ch16 m23:: <i>ura4</i> -TEL[72]	<i>h</i> ^A	<i>leu1-32, ade6-210, ura4-DS/E (Ch16 ade6-216) rik1-304</i>
FY611	Ch16 m23:: <i>ura4</i> -TEL[72]	<i>h</i> ^A	<i>leu1-32, ade6-210, ura4-DS/E (Ch16 ade6-216) swi6-115</i>
FY521	Ch16 m23:: <i>ura4</i>	<i>h</i> ⁻	<i>leu1-32, ade6-210, ura4-DS/E (Ch16 ade6-216)</i>
FY721	Ch16 m23:: <i>ura4</i>	<i>h</i> ⁻	<i>leu1-32, ade6-210, ura4-DS/E (Ch16 ade6-216)</i>
FY723	Ch16 m23:: <i>ura4</i>	<i>h</i> ^A	<i>leu1-32, ade6-210, ura4-DS/E (Ch16 ade6-216) clr1-5</i>
FY725	Ch16 m23:: <i>ura4</i>	<i>h</i> ^A	<i>leu1-32, ade6-210, ura4-DS/E (Ch16 ade6-216) clr2-E22</i>
FY727	Ch16 m23:: <i>ura4</i>	<i>h</i> ^A	<i>leu1-32, ade6-210, ura4-DS/E (Ch16 ade6-216) clr3-E36</i>

Table 2. (Continued)

Strain	Position and <i>ura4</i> gene	Genotype
FY729	Ch16 m23:: <i>ura4</i>	<i>h^A leu1-32, ade6-210, ura4-DS/E</i> (Ch16 <i>ade6-216</i>) <i>clr4-S5</i>
FY731	Ch16 m23:: <i>ura4</i>	<i>h^A leu1-32, ade6-210, ura4-DS/E</i> (Ch16 <i>ade6-216</i>) <i>rik1-304</i>
FY733	Ch16 m23:: <i>ura4</i>	<i>h^A leu1-32, ade6-210, ura4-DS/E</i> (Ch16 <i>ade6-216</i>) <i>swi6-115</i>
FY1036	Ch16 m23:: <i>ura4</i>	<i>h^A leu1-32, ade6-210, ura4-DS/E</i> (Ch16 <i>his1-102</i>) <i>swi6Δ::his1⁺</i>
FY757		<i>h⁺ ade6-704, (CM3112 sup3-5)</i>
FY759		<i>h⁻ ade6-704, (CM3112 sup3-5)</i>
FY853		<i>h^A ade6-704, (CM3112 sup3-5) clr1-5</i>
FY787		<i>h^A ade6-704, (CM3112 sup3-5) clr2-E22</i>
FY790		<i>h^A ade6-704, (CM3112 sup3-5) clr3-E36</i>
FY856		<i>h^A ade6-704, (CM3112 sup3-5) clr4-S5</i>
FY859		<i>h^A ade6-704, (CM3112 sup3-5) rik1-304</i>
FY862		<i>h^A ade6-704, (CM3112 sup3-5) swi6-115</i>
FY1038		<i>h^A ade6-704, (CM3112 sup3-5) his1-102 swi6Δ::his1⁺</i>

(*h^A*) Mating type is ambiguous because the silent mating-type loci are deregulated in this background.

tions were performed as in Allshire et al. (1994). Probes were gel-purified using GeneClean (Bio101) or Wizard DNA Clean-up (Promega). A 1.4-kb *Hind*III fragment containing the deleted (*ura4-DS/E*) version of the *ura4⁺* gene was used to hybridize DNA and RNA filters. A 300-bp *Hpa*I-*Xho*I fragment from the Phe-*otr1* region of *cen1* was used to distinguish left and right side *ura4⁺* insertions in the Phe-*otr/dh/k'* region of *cen1*. A PCR product, 208, from the middle of *imr1* was used to distinguish left and right side insertions in the *imr1/cnt1* (B'/CC1) region.

RNA preparation and analyses

RNA was prepared and analyzed as described previously (Allshire et al. 1994). Quantitation of *ura4⁺* and *ura4-DS/E* mRNA levels was performed using a Molecular Dynamics PhosphorImager and Image Quantification software. The automatic background measuring device was turned off, and the background signal in each track was determined by volume integration of a region, equal in size to that used to measure the volume of the *ura4⁺* and *ura4-DS/E* signals in each track. Subsequently, this background reading was manually deducted from the other measurements in that track.

Acknowledgments

We thank W. Bickmore, D. Broccoli, H. Cooke, N. Hastie, D. Kipling, P. Lord, D. Young, and other members of Chromosome Biology for valuable discussion and comments on the manuscript and N. Davidson, S. Bruce, and D. Stewart for photographic and art work. We also acknowledge A. Klar, R. Egel, and H. Schmidt for providing the *clr1-5*, *rik1-304*, and *swi6-115* mutant strains, respectively. This work was supported by the Medical Research Council of Great Britain. J-P.J. was supported by a Wellcome Trust Fellowship. K.E. was and is supported by a European Molecular Biology Organization Long-Term Fellowship and a Human Science Frontier Program Fellowship, respectively.

The publication costs of this article were defrayed in part by payment of page charges. This article must therefore be hereby marked "advertisement" in accordance with 18 USC section 1734 solely to indicate this fact.

References

- Allshire, R.C. 1992. Manipulation of large minichromosomes in *Schizosaccharomyces pombe* with liposome-enhanced transformation. *Methods Enzymol.* **216**: 614–631.
- Allshire, R.C., J.-P. Javerzat, N.J. Redhead, and G. Cranston. 1994. Position effect variegation at fission yeast centromeres. *Cell* **76**: 157–169.
- Aparicio, O.M., B.L. Billington, and D.E. Gottschling. 1991. Modifiers of position effect are shared between telomeric and silent mating-type loci in *S. cerevisiae*. *Cell* **66**: 1279–1287.
- Baska, K., H. Morawietz, V. Dombradi, M. Axton, H. Taubert, G. Szabo, I. Torok, A. Udvary, H. Gyurkovics, B. Szoor, D. Glover, G. Reuter, and J. Gausz. 1993. Mutations in the protein phosphatase 1 gene at 87B can differentially affect suppression of position-effect variegation and mitosis in *Drosophila melanogaster*. *Genetics* **135**: 117–125.
- Bell, S.P., R. Kobayashi, and B. Stillman. 1993. Yeast origin recognition complex functions in transcription silencing and DNA replication. *Science* **262**: 1844–1849.
- Bernat, R.L., M.R. Delannoy, N.F. Rothfield, and W.C. Earnshaw. 1991. Disruption of centromere assembly during interphase inhibits kinetochore morphogenesis and function in mitosis. *Cell* **66**: 1229–1238.
- Butner, K. and C. Lo. 1986. Modulation of *tk* expression in mouse pericentromeric heterochromatin. *Mol. Cell. Biol.* **6**: 4440–4449.
- Chung, J.H., M. Whiteley, and G. Felsenfeld. 1993. A 5' element of the chicken beta-globin domain serves as an insulator in human erythroid cells and protects against position effect in *Drosophila*. *Cell* **74**: 505–514.
- Clarke, L., M. Baum, L.G. Marschall, V.K. Ngan, and N.C. Steiner. 1993. Structure and function of *Schizosaccharomyces pombe* centromeres. *Cold Spring Harbor Symp. Quant. Biol.* **58**: 687–695.
- Cooke, C.A., R.L. Bernat, and W.C. Earnshaw. 1990. CENP-B: A major human centromere protein located beneath the kinetochore. *J. Cell Biol.* **110**: 1475–1488.
- Dorer, D.R. and S. Henikoff. 1994. Expansions of transgene repeats cause heterochromatin formation and gene silencing in *Drosophila*. *Cell* **77**: 993–1002.
- Earnshaw, W.C., H. Ratrie, and G. Setten. 1989. Visualisation of centromere proteins CENP-B and CENP-C on stable dicen-

- tric chromosomes in cytological spreads. *Chromosoma* **98**: 1–12.
- Egel, R., M. Willer, and O. Nielsen. 1989. Unblocking of meiotic crossing-over between the silent mating-type cassettes of fission yeast, conditioned by the recessive, pleiotropic mutant *rik1*. *Curr. Genet.* **15**: 407–410.
- Eissenberg, J.C. 1989. Position effect variegation in *Drosophila*: Towards a genetics of chromatin assembly. *BioEssays* **11**: 14–17.
- Eissenberg, J.C., G.D. Morris, G. Reuter, and T. Hartnett. 1992. The heterochromatin-associated protein HP-1 is an essential protein in *Drosophila* with dosage dependent effects on position effect variegation. *Genetics* **131**: 345–352.
- Ekwall, K. and T. Ruusala. 1994. Mutations in *rik1*, *clr2*, *clr3* and *clr4* genes asymmetrically derepress the silent mating-type loci in fission yeast. *Genetics* **136**: 53–64.
- Ferguson, M. and D.C. Ward. 1992. Cell cycle dependent chromosomal movement in pre-mitotic human T-lymphocyte nuclei. *Chromosoma* **101**: 557–565.
- Foss, M., F.J. McNally, P. Laurenson, and J. Rine. 1993. Origin recognition complex (ORC) in transcriptional silencing and DNA replication in *S. cerevisiae*. *Science* **262**: 1838–1844.
- Funabiki, H., I. Hagan, S. Uzawa, and M. Yanagida. 1993. Cell cycle dependent specific positioning and clustering of centromeres and telomeres in fission yeast. *J. Cell Biol.* **121**: 961–976.
- Gottschling, D.E. 1992. Telomere-proximal DNA in *Saccharomyces cerevisiae* is refractory to methyltransferase activity in vivo. *Proc. Natl. Acad. Sci.* **89**: 4062–4065.
- Gottschling, D.E., O.M. Aparicio, B.L. Billington, and V.A. Zakian. 1990. Position effect at *S. cerevisiae* telomeres: Reversible repression of Pol II transcription. *Cell* **63**: 751–762.
- Haaf, T., P.E. Warburton, and H.F. Willard. 1992. Integration of human α -satellite DNA into Simian chromosomes: Centromere protein binding and disruption of normal chromosome segregation. *Cell* **70**: 681–696.
- Hahnenberger, K.M., J. Carbon, and L. Clarke. 1991. Identification of DNA regions required for mitotic and meiotic functions within the centromere of *Schizosaccharomyces pombe* chromosome 1. *Mol. Cell. Biol.* **11**: 2206–2215.
- Henikoff, S. 1990. Position effect variegation after 60 years. *Trends Genet.* **6**: 422–426.
- . 1994. A reconsideration of the mechanism of position effect. *Genetics* **138**: 1–5.
- Heyer, W.D., M. Sipiczki, and J. Kohli. 1986. Replicating plasmids in *Schizosaccharomyces pombe*: Improvement of symmetric segregation by a new genetic element. *Mol. Cell. Biol.* **6**: 80–89.
- Hochstrasser, M., D. Mathog, Y. Gruenbaum, H. Saumweber, and J.W. Sedat. 1986. Spatial organization of chromosomes in the salivary gland nuclei of *Drosophila melanogaster*. *J. Cell Biol.* **102**: 112–123.
- Karpen, G. 1994. Position-effect variegation and the new biology of heterochromatin. *Curr. Opin. Genet. Dev.* **4**: 281–291.
- Kellum, R. and P. Schedl. 1991. A position-effect assay for boundaries of higher order chromosomal domains. *Cell* **64**: 941–950.
- Kipling, D. and S.E. Kearsley. 1990. Reversion of autonomously replicating sequence mutations in *Saccharomyces cerevisiae*: Creation of a eukaryotic replication origin within prokaryotic vector DNA. *Mol. Cell. Biol.* **10**: 265–272.
- Klein, F., T. Laroche, M.E. Cardenas, J.F.X. Hofmann, D. Schweitzer, and S. Gasser. 1992. Localisation of RAP1 and Topoisomerase II in nuclei and meiotic chromosomes of yeast. *J. Cell Biol.* **117**: 935–948.
- Kyrion, G., K. Liu, C. Liu, A.J. Lustig. 1993. RAP1 and telomere structure regulate telomere position effects in *Saccharomyces cerevisiae*. *Genes & Dev.* **7**: 1146–1159.
- Larin, Z., M.D. Fricker, and C. Tyler-Smith. 1994. De novo formation of several features of a centromere following introduction of a Y alphoid YAC into mammalian cells. *Hum. Mol. Genet.* **3**: 689–695.
- Laurenson, P. and J. Rine. 1992. Silencers, silencing and heritable transcriptional states. *Microbiol. Rev.* **56**: 543–560.
- Lorentz, A., K. Ostermann, O. Fleck, and H. Schmidt. 1994. Switching gene *swi6*, involved in repression of silent mating-type loci in fission yeast, encodes a homologue of chromatin-associated proteins from *Drosophila* and mammals. *Gene* **143**: 139–143.
- Matsumoto, T., S. Murakami, O. Niwa, M. Yanagida. 1990. Construction and characterization of centric and acentric linear minichromosomes in fission yeast. *Curr. Genet.* **18**: 323–330.
- Micklem, G., A. Rowley, J. Harwood, K. Nasmyth, and J.F.X. Diffley. 1993. Yeast origin recognition complex is involved in DNA replication and transcriptional silencing. *Nature* **366**: 87–89.
- Miklos, G.L. and J.N. Cotsell. 1990. Chromosome structure at interfaces between major chromatin types: Alpha- and beta-heterochromatin. *Bioessays* **21**: 1–6.
- Moreno, S., A. Klar, and P. Nurse. 1991. Molecular genetic analysis of fission yeast *Schizosaccharomyces pombe*. *Methods Enzymol.* **194**: 795–823.
- Murakami, S., T. Matsumoto, O. Niwa, and Yanagida, M. 1991. Structure of the fission yeast centromere *cen3*: Direct analyses of the reiterated inverted region. *Chromosoma* **101**: 214–221.
- Nakaseko, Y., Y. Adachi, S. Funahashi, O. Niwa, and M. Yanagida. 1986. Chromosome walking shows a highly homologous repetitive sequence present in all the centromere regions of fission yeast. *EMBO J.* **5**: 1011–1021.
- Nicol, L. and P. Jeppesen. 1994. Human autoimmune sera recognize a conserved 26 kD protein associated with heterochromatin that is homologous to heterochromatin protein 1 of *Drosophila*. *Chromosome Res.* **2**: 245–255.
- Nimmo, E.R., G. Cranston, and R.C. Allshire. 1994. Telomere associated breakage in fission yeast results in variegated expression of adjacent genes. *EMBO J.* **13**: 3801–3811.
- Niwa, O., T. Matsumoto, Y. Chikashige, and M. Yanagida. 1989. Characterization of *Schizosaccharomyces pombe* minichromosome deletion derivatives and a functional allocation of their centromere. *EMBO J.* **8**: 3045–3052.
- Palladino, F., T. Laroche, E. Gilson, A. Axelrod, L. Pillus, and S.M. Gasser. 1993. SIR3 and SIR4 proteins are required for the positioning and integrity of yeast telomeres. *Cell* **75**: 543–555.
- Paro, R. 1993. Mechanisms of heritable gene repression during development of *Drosophila*. *Curr. Opin. Cell Biol.* **5**: 999–1005.
- Paro, R. and D.S. Hogness. 1991. The polycomb protein shares a homologous domain with a heterochromatin-associated protein of *Drosophila*. *Proc. Natl. Acad. Sci.* **88**: 263–267.
- Polizzi, C.M. and L. Clarke. 1991. The chromatin structure of centromeres from fission yeast is distinct, with a differentiation of the central core which correlates with function. *J. Cell Biol.* **112**: 191–201.
- Powers, J.A. and J.C. Eissenberg. 1993. Overlapping domains of the heterochromatin-associated protein HP1 mediate nuclear localization and heterochromatin binding. *J. Cell Biol.* **120**: 291–299.
- Rattner, J.B. 1991. The structure of the mammalian chromo-

- some. *Bioessays* **13**: 51–56.
- Saunders, W.S., C. Chue, M. Goebel, C. Craig, R.F. Clark, J.A. Powers, J.C. Eissenberg, S.C. Elgin, N.F. Rothfield, and W.C. Earnshaw. 1993. Molecular cloning of a human homologue of *Drosophila* heterochromatin protein HP1 using anti-centromere autoantibodies with anti-chromo specificity. *J. Cell Sci.* **104**: 573–582.
- Singh, J. and A.J.S. Klar. 1992. Active genes in budding yeast display enhanced *in vivo* accessibility to foreign DNA methylases: A novel *in vivo* probe for chromatin structure of yeast. *Genes & Dev.* **6**: 186–196.
- Singh, P.B., J.R. Miller, J.J. Pearce, R.D. Burton, R. Paro, T.C. James, and S.J. Gaunt. 1991. A sequence motif found in a *Drosophila* heterochromatin protein is conserved in animal and plants. *Nucleic Acids Res.* **19**: 789–793.
- Steiner, N.C. and L. Clarke. 1994. A novel epigenetic effect can alter centromere function in fission yeast. *Cell* **79**: 865–874.
- Steiner, N.C., K.M., Hahnenberger, and L. Clarke. 1993. Centromeres of the fission yeast *Schizosaccharomyces* are highly variable genetic loci. *Mol. Cell. Biol.* **13**: 4578–4587.
- Takahashi, K., S. Murakami, Y. Chikashige, H. Funabiki, O. Niwa, and M. Yanagida. 1992. A low copy number central sequence with strict symmetry and unusual chromatin structure in the fission yeast centromere. *Mol. Biol. Cell.* **3**: 819–835.
- Thon, G. and A.J.S. Klar. 1992. The *clr1* locus regulates the expression of the cryptic mating-type loci in fission yeast. *Genetics* **131**: 287–296.
- . 1993. Directionality of fission yeast mating-type interconversion is controlled by the location of the donor loci. *Genetics* **134**: 1045–1054.
- Thon, G., A. Cohen and A.J.S. Klar. 1994. Three additional linkage groups that repress transcription and meiotic recombination in the mating-type region of *Schizosaccharomyces pombe*. *Genetics* **138**: 29–38.
- Tyler-Smith, C. and H.F. Willard. 1993. Mammalian chromosome structure. *Curr. Opin. Genet. Dev.* **3**: 390–397.
- Vourc'h, C., D. Taruscio, A.L. Boyle, and D.C. Ward. 1993. Cell cycle-dependent distribution of telomeres, centromeres, and chromosome-specific subsatellite domains in the interphase nucleus of mouse lymphocytes. *Exp. Cell. Res.* **205**: 142–151.
- Wines, D.R. and S. Henikoff. 1992. Instability of a *Drosophila* chromosome. *Genetics* **131**: 683–691.
- Wreggett, K.A., F. Hill, P.S. James, A., Hutchings, G.W. Butcher, and P.B. Singh. 1994. A mammalian homologue of *Drosophila* heterochromatin protein 1 (HP1) is a component of constitutive heterochromatin. *Cytogenet. Cell Genet.* **66**: 99–103.



Mutations derepressing silent centromeric domains in fission yeast disrupt chromosome segregation.

R C Allshire, E R Nimmo, K Ekwall, et al.

Genes Dev. 1995, **9**:

Access the most recent version at doi:[10.1101/gad.9.2.218](https://doi.org/10.1101/gad.9.2.218)

References

This article cites 63 articles, 29 of which can be accessed free at:
<http://genesdev.cshlp.org/content/9/2/218.full.html#ref-list-1>

License

Email Alerting Service

Receive free email alerts when new articles cite this article - sign up in the box at the top right corner of the article or [click here](#).

